

Simulations of CVD Diamond Film Growth Using a Simplified Monte Carlo Model

Paul W. May¹, Jeremy N. Harvey¹, Neil L. Allan¹, James C. Richley¹ and Yuri M. Mankelevich²

¹School of Chemistry, University of Bristol, Bristol BS8 1TS, United Kingdom.

²Skobel'tsyn Institute of Nuclear Physics, Moscow State University, Vorob'evy gory, Moscow 119991, Russia.

ABSTRACT

A simple 1-dimensional kinetic Monte Carlo (KMC) model has been developed to simulate the chemical vapour deposition (CVD) of a diamond (100) surface. The model considers adsorption, etching/desorption, lattice incorporation, and surface migration along and across the dimer rows. The reaction probabilities for these processes are re-evaluated in detail and their effects upon the predicted growth rates and morphology are described. We find that for standard CVD diamond conditions, etching of carbon species from the growing surface is negligible. Surface migration occurs rapidly, but is mostly limited to CH₂ species oscillating rapidly back and forth between two adjacent radical sites. Despite the average number of migration hops being in the thousands, the average surface diffusion length for a surface species before it either adds to the diamond lattice or is removed back to the gas phase is <2 sites.

INTRODUCTION

Chemical vapour deposition (CVD) of diamond is a maturing technology that is beginning to find many commercial applications in electronics, cutting tools, medical coatings and optics [1]. The CVD process involves the gas phase decomposition of a gas mixture containing a small quantity of a hydrocarbon in excess hydrogen [2]. A typical gas mixture uses CH₄ in H₂ (plus sometimes additional Ar or N₂), and depending upon the growth conditions, substrate properties and growth time, this produces polycrystalline films with grain sizes from ~5 nm to mm. Films with grain sizes less than 10-20 nm are often called ultrananocrystalline diamond films, UNCD; those with grain sizes a few 10s or 100s of nm are nanocrystalline diamond films (NCD); those with grain sizes microns or tens of microns are termed microcrystalline diamond films (MCD) range; and those with grain sizes approaching 1 mm are single crystal diamond (SCD).

However, to obtain a diamond film with the desired morphology combined with controlled electronic and mechanical properties requires a detailed understanding of the many parameters affecting growth, such as the substrate temperature, gas mixture, process pressure, *etc.* The difficulty with this is that, even 20 years after diamond CVD was first developed, the exact details of the growth mechanism remain controversial. The so-called 'standard growth mechanism' [3] developed in the early 1990s is a reasonably robust description of the general CVD diamond process. In this model, atomic H, created by thermal or electron-impact dissociation of H₂, is the driving force behind all the chemistry. It is widely accepted [4,5] that the main growth species in standard diamond CVD is the CH₃ radical, which adds to the diamond surface following hydrogen abstraction by H atoms. An elevated substrate temperature (typically >700°C) allows migration of the adsorbed C species until they meet a step-edge and

add to the diamond lattice. Another role for the atomic H is to etch back into the gas phase any adsorbed carbon groups that have deposited as non-diamond phases. It is believed that hydrocarbons C_xH_y with 2 or more carbons ($x \geq 2$) are prevented from contributing to the growth by the 'β-scission' reaction which is a rapid, low energy, efficient process that stops the build up of polymer chains on the growing surface. Diamond growth is therefore seen as competition between etching and deposition, with carbons being added to the diamond on an atom-by-atom basis.

Our group recently developed a modified version of the standard growth model which considers the effects of all the C_1 hydrocarbon radicals (CH_3 , CH_2 , CH and C atoms) on both monoradical and biradical sites on a (100) diamond surface [6]. Our growth model also relies upon surface migration of CH_2 groups along and across the reconstructed dimer rows in order to predict growth rates to within a factor of two of experimental observations. Using the model we derived expressions for the fraction of surface radical sites based upon the substrate temperature, T_s , and the concentrations of H and H_2 above the surface. Under typical CVD diamond conditions with $T_s \sim 900^\circ C$ and 1% CH_4/H_2 around 10% of the surface carbon atoms support radical sites.

Despite these successes, evidence for surface migration, nucleation processes, the effects of gas impurities and gas-surface reactions are sparse and mostly circumstantial. To investigate these ideas we developed a simplified one-dimensional Monte Carlo (MC) model of the growth of diamond films [7] for a fixed set of process conditions and substrate temperature. Although the model was only 1D, the interplay between adsorption, etching/desorption and addition to the lattice was modelled using known or estimated values for the rates of each process. For typical CVD diamond conditions, the model predicted growth rates of $\sim 1 \mu m h^{-1}$, consistent with experiment. Various other growth processes were also predicted, such as step-edge growth, a large positive value for the Ehrlich-Schwoebel potential for migrating species attempting to migrate off the top of step-edges leading to atomic-scale 'wedding cake' structures, and it also showed that β-scission is not as important for determining the surface morphology as previously envisaged.

In a follow-up paper [8], we modelled surface defects by assigning values for the probability of their appearance following certain surface processes, such as migration and adsorption. Such immobile, unetchable surface defects acted as critical nuclei, allowing the nucleation of new layers, and thus a greatly increased growth rate when the rate-determining step for growth is new layer nucleation. The defects also instigate the (re)nucleation of a new crystallite, ultimately leading to a polycrystalline film. We showed that using these ideas, we could qualitatively model columnar growth of MCD films, as well as NCD and UNCD morphologies.

However, these MC models relied heavily upon the kinetic parameters for the various surface process reported in the literature. To extend the MC model further, for example to include temperature dependence, it was necessary to re-examine these values to determine their accuracy and consistency with the microscopic rates for elementary processes at the diamond surface. In this paper we shall re-examine the processes of CH_3 adsorption, surface migration, and etching and try to rationalise models for their temperature dependent rates which will then be used in a new version of the MC program.

THEORETICAL METHODS

The original model for the MC program is given in detail in refs.[7] and [8] and therefore we shall give only a brief description here, along with new additions and modifications. In our MC model, the (100) diamond lattice is represented in only 2 dimensions, as a cross-section, with the top (growing) surface positioned towards the top of the screen. Each C atom is represented by a square block within the lattice, with different coloured blocks representing different ‘types’ of carbon bonding. Carbons that are fully bonded into the bulk diamond lattice are coloured dark-blue whereas carbons that form the surface layer are coloured grey. Green blocks are used to represent pendant CH_3 groups or bonded CH_2 structures that bridge along or across the rows of the dimer pairs on the reconstructed (100) surface, and these are immobile. A new modification is that now we allow an immobile green block to become ‘activated’ following a successful H-abstraction reaction. Such activated blocks are coloured red, and are allowed to migrate to a neighbouring block, so long as there is a surface radical site present. This change has been implemented because computational models of carbon migration [9,10] suggest that dual activation of the migrating and neighbouring sites is required. A surface radical site is coloured magenta, and occurs as a result of a grey block being activated by a successful H abstraction (see figure 1).

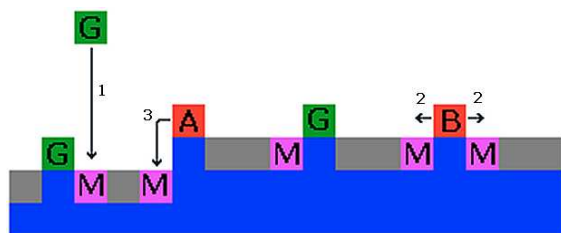


Figure 1. A schematic diagram of the model for the cross-section of the diamond surface and some of the processes. Magenta blocks (M) represent activated surface radical sites. The unlabelled light-grey blocks represent unactivated, unreactive (hydrogenated) surface sites, while dark-blue blocks represent bulk (sub-surface) diamond. Green blocks (G) represent immobile CH_3 or CH_2 groups created as a result of adsorption of CH_3 from the gas phase onto M sites (process labelled 1). The red blocks (A and B) represent activated CH_2 groups that are able to migrate. In process 2, red block B can jump left or right since there is an M block at either site. In process 3, red block A cannot jump right since there is no M block there. But it can jump left and drop down the step-edge (following the ‘lemmings’ scenario [6]) since there is an available M block at the corner.

The grid has a maximum size of 600×400 . At the start of the program, a flat horizontal surface of grey blocks is defined at the bottom of the screen to represent the surface of a single crystal diamond substrate. This new version of the program is now fully stochastic (so that the MC program may now be considered a true KMC model), and operates by comparing the relative rates of each process rather than the probabilities of each processes occurring compared to the fastest in previous versions. The program now generates a random number, R ($0 \leq R < 1$), so that at each simulation step a process is chosen with a probability proportional to its rate.. The randomly chosen process is carried out, along with any consequences, and a new list of possible

processes is generated ready for the next random number comparison. The processes involved are:

- (a) Surface site activation. A grey surface block is activated by H abstraction to form a surface radical site. The grey block then turns magenta, and this square is now available for adsorption of an incoming green or a migrating red block.
- (b) Surface site deactivation. This is the opposite to (a), in that a magenta surface radical site is deactivated by H addition to become a standard unreactive grey surface site.
- (c) Adsorption of a CH₃ group onto a surface radical site. In this case a new incoming green-coloured block is chosen at a random horizontal position corresponding to one of the activated surface sites (red or magenta) at the top of the screen, and then allowed to drop vertically until it meets the surface, whereupon it temporarily adsorbs at this position. This block represents a generic C₁ adsorbing unit, which is most probably CH₃ but could be species such as C, CH, CH₂ or even CN, as favourable processes for addition of these species to activated sites exist. (In fact, C, CH and ¹CH₂ can undergo facile processes for addition even to an *unactivated* (grey) site [11] but these processes do not play a major role under the present conditions.) The adsorbed green block then has a number of possible pathways (d)-(h), depending upon the local morphology where it landed, and each possible fate is included in the list of possible processes. One other possible fate for it is to stick permanently to form a static, unetchable defect – however, in the work described here we have turned off this option since we are focusing upon the other processes.
- (d) Etching. Isolated CH₂ bridging units or CH₃ groups may be etched back into the gas phase following H abstraction reactions. The green block is then removed and forgotten by the program.
- (e) Activation. As a result of a subsequent H abstraction, the CH₃ becomes an activated CH₂ group (and the green block turns red) which is now capable of migration.
- (f) Deactivation. As a result of H addition onto an activated CH₂ group, the group is ‘deactivated’ and returns to being an immobile (green) CH₂ bridge or pendant CH₃.
- (g) Migration. An activated (red) CH₂ block may jump sideways left or right one position, so long as there is a (magenta) radical site available to jump into. If migration occurs, the block jumps to the neighbouring site (and remains red), and the site it previously occupied now become magenta, since this is now an activated surface site.
- (h) Addition to the lattice. If an adsorbing block lands adjacent to a step edge, it will fuse to the lattice and turn grey [12]. This is an example of an Eley-Rideal-type process (ER). Alternatively, if a migrating red block jumps and lands next to a step-edge, it too may fuse to the lattice and turn grey. This is a Langmuir-Hinshelwood-type process (LH).
- (i) Once a block is no longer part of the surface layer, *i.e.* it has been buried beneath at least one other layer it turns dark-blue to represent the bulk lattice.

Three other features of the model need to be mentioned. First, this 1D model assumes that the ‘normal critical nucleus’ for diamond growth is two adjacent blocks. This is defined as the smallest immobile, unetchable surface feature that provides step-edges suitable for propagating layer growth. Under standard growth conditions a normal 2-block critical nucleus can be formed by (i) an ER-type process, where an incoming green block adsorbs directly next to a previously adsorbed block causing both of them to bond together, or (ii) a LH-type process where an adsorbed red block migrates next to a green or red block and they fuse together. These two processes form the basis for new layer nucleation in the absence of defects.

Second, β -scission is modelled by scanning the surface blocks after every time-step and identifying and deleting any 2-block pillars that may have arisen as a result of blocks landing or migrating.

Finally, there is the issue of blocks migrating off the top of step-edges. Previously, [7,8] we adopted the ‘cowards’ scenario as the default process, which meant that migrating blocks could not jump off the top of step-edges, consistent with a positive Ehrlich-Schwoebel barrier for this process. However, recent quantum mechanical calculations [13] suggest that this barrier is much smaller than previously thought, and is of a similar magnitude to the barrier for migration on a flat surface. Therefore we have now adopted the ‘lemmings’ scenario as the default process, whereby migrating (red) blocks can readily jump off the step-edge and ‘fall’ to the bottom (which may be several blocks in height), landing in the bottom corner (so long as the surface block beneath is activated, *i.e.* magenta). The block then fuses to the lattice at this corner.

The program was run until it was stopped manually or until a preset number of layers (typically 300 to provide statistical invariance) had grown, at which point the data were saved. Depending upon the input parameters for the various events, the program took several hours to grow 300 layers (on a Pentium 4 PC). At each step the time taken was updated according to $t_{\text{new}} = t_{\text{old}} - \ln(R)/S$, where t_{old} is the cumulative time up to the previous step, R is a random number ($0 \leq R < 1$), and S is the sum of the rates of all possible processes [14]. Thus, the growth rate can be calculated since in the simulation 300 layers of diamond grew in this time, with the average C-C distance along a (100) diamond face (*i.e.* 1 block) being 0.0892 nm.

In this paper the growth conditions were fixed for standard polycrystalline CVD grown using 1%CH₄/H₂ at a process pressure of ~20 Torr but with varying temperatures [6]. We shall now reinvestigate each of the processes in turn.

CH₃ adsorption

In previous papers we have described a model for the gas chemistry occurring within hot filament or microwave plasma CVD reactors [6,15]. This model has been tested against laser spectroscopy and *in situ* mass spectrometric measurements. For a given set of process conditions we can use this model to determine, with reasonable accuracy, the concentrations of all the major gas phase species at any position within the reactor. Thus, we can extract the concentration of CH₃ just above the growing surface and extrapolate this to determine the rate of CH₃ species striking the surface per second. The number of CH₃ impacts cm⁻² s⁻¹ is given by $[\text{CH}_3]_s \times v/4$, where $v = 3757 \times T_{\text{ns}}^{0.5}$ (cm s⁻¹) is the mean thermal velocity of CH₃ and T_{ns} is the gas temperature near the substrate surface. However, most of these impacts will be with a hydrogenated surface C, and so the CH₃ will simply bounce off. Only those impacts which strike dangling bonds will be important for growth and need be considered in the model. We shall ignore the effects of co-adsorbed dopant atoms on the adsorption rate, since this is beyond the scope of the present work [16]. Assuming that the gas temperature near the surface, T_{ns} , is approximately the same as the surface temperature, T_s , and that 1 cm² of the diamond surface contains $\sim 1.56 \times 10^{15}$ C atoms, then the rate at which CH₃ species strike the surface site (in s⁻¹) is given by:

$$\text{CH}_3 \text{ impact rate} = \{P \times [\text{CH}_3]_s \times (3757 \times \sqrt{T_{\text{ns}}}) / 4\} / 1.56 \times 10^{15} \quad (1)$$

where P is the probability of adsorption onto a radical site (*i.e.* the sticking probability). The value of P results from a combination of factors that reduce the reaction probability, such as a geometrical factor (g) due to unfavourable collision orientation and a steric-electronic factor (s), such that:

$$P = g \times s \quad (2)$$

The factor s can be estimated since it is known from electronic spin statistics that, on average, 3 collisions out of 4 will be on the triplet surface and will not lead to reaction at the high temperatures of diamond CVD [17], and that not all of the surface radical sites will be accessible for adsorption (roughly 50%). This leads to an estimated value for s of ~ 0.15 . For the standard hot filament deposition conditions [6] used in this paper [CH_3] $_s = 1.4 \times 10^{13} \text{ cm}^{-3}$, [H] $_s = 1.85 \times 10^{14} \text{ cm}^{-3}$, $T_{\text{ns}} \sim T_s = 1173 \text{ K}$ and $g = 0.5$, giving a per site rate of CH_3 impact of $\sim 20 \text{ s}^{-1}$. This rate is then multiplied by the number of surface radical sites (red + magenta) available at that time-step to obtain the total relative adsorption rate.

Etching

The etching of diamond in atomic H atmospheres is known to be very slow ($0.2\text{--}0.5 \text{ nm h}^{-1}$ [18]), but nevertheless has been proposed as a mechanism by which surface smoothing occurs during growth [19]. For our MC model, we require the etching rate for an isolated surface CH_2 or CH_3 group, which may be higher than that of the bulk lattice. Simple thermal desorption has been discounted as a removal mechanism due to the relatively low substrate temperatures and the high C–C bond energy. Previously, to obtain a value for the etch rate we followed Netto & Frenklach [20] and assumed that the etching step is simply the reverse of the CH_3 addition process. Here, an adsorbed CH_2 group is removed back into the gas phase (catalysed by H) as CH_3 , leaving behind a surface dangling bond. Netto & Frenklach calculated two etch rates for the two types of bridging site (termed A3 and A4 in refs.[9] & [21]), which we previously averaged [7] to get a mean etch rate.

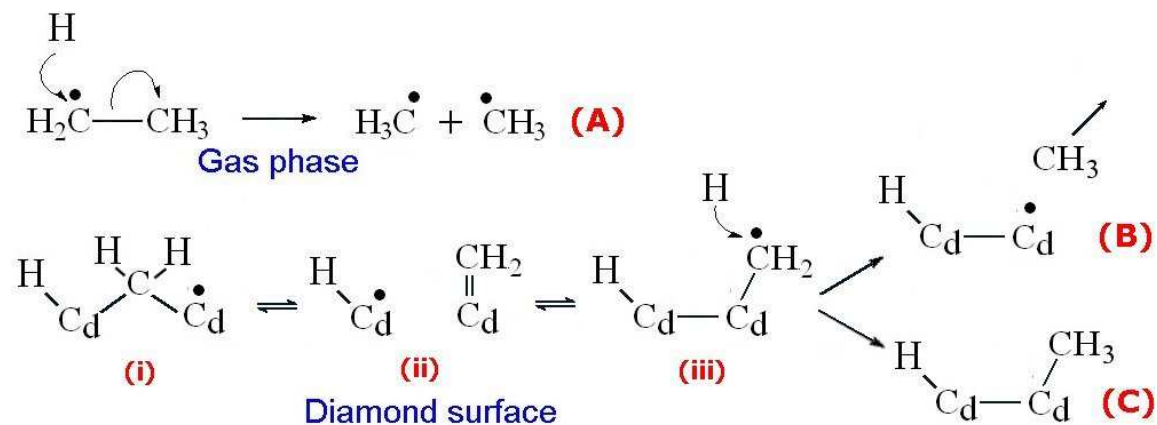


Figure 2. Comparison of the proposed CH_3 etching mechanism on a diamond surface (B) & (C) with an analogous gas phase reaction (A). C_d is carbon in the diamond lattice.

However, the problem with these etch rates is that the assumptions used by Skokov *et al.* [9] in their derivation are questionable. These authors assumed that the H addition reaction to gas phase CH₂CH₃ (figure 2, reaction (A)) is a reasonable analogy to those occurring on the diamond surface (figure 2, reactions (B) & (C)), and thus that the known rate for the former reaction could be used as a good approximation to the etching rate. However, in a gas phase reaction such as this, the excess vibrational energy deposited in the molecule due to formation of a C–H bond can only escape due to relatively slow radiative or collisional processes, with unimolecular decay due to C–C bond cleavage and hence the formation of CH₃ dominating. But on the diamond surface, the heat released by addition of H to the CH₂ group can rapidly be dissipated into the bulk (reaction (C)), so that only prompt C–C bond cleavage (reaction (B)) can compete with vibrational deactivation. The rate of etching (B) will be proportional to the relative lifetime of state (iii), which is small in comparison with the more probable state (i). The rate will also be related to the proportion of the deposited energy which remains close to the surface in state (iii) compared to that dissipated within the timescale required to break the C–C bond. Hence the efficiency of etching by this mechanism can be seen to be inversely dependent on the thermal conductivity of the diamond surface. Diamond has a very high thermal conductivity, and so energy dissipation is likely to be rapid – however, it is not clear if the thermal conductivity in the near-surface region would be as large as that of bulk diamond. Nevertheless, it is likely that the rate of loss of CH₃ would be reduced to such an extent that etching by this mechanism may be essentially negligible (consistent with both the low etch rates [18] and the low values (<10⁻⁶) of sputtering yield of C atoms per H atoms seen experimentally [22]). Therefore, previous MC models (both ours and others [20,23]) may have significantly over-estimated the etch rates and therefore the importance of etching in controlling surface morphology and growth processes. Work is currently underway to calculate the etch rate using molecular dynamics modelling of the bond breaking and energy dissipation processes, but meanwhile, we have assumed that etching can only occur by direct breaking of the C–C bond. To model this we used an Arrhenius expression for the rate constant for etching

$$k_{\text{etch}} = A_{\text{etch}} \exp(-E_a / RT_s) \quad (3)$$

where A_{etch} is the collision frequency which we have assumed is the same as that used by Netto & Frenklach (10¹³ s⁻¹), E_a is the activation energy which we have taken to be equivalent to the C–C bond energy (348 kJ mol⁻¹), R is the gas constant and T_s is the substrate temperature. With $T_s = 1173$ K, this gives the per site etching rate as 3×10^{-3} s⁻¹, which is a factor of 1000× slower than most other processes, confirming the notion that such etching processes are almost negligible.

CH₂ activation and deactivation

From [20], the rate of creation of surface radicals due to of H abstraction is given by

$$\text{Activation rate (s}^{-1}\text{)} = k_1 [\text{H}]_s U \quad (4)$$

with the rate constant $k_1 = 8.63 \times 10^{-11} \exp(-3360/T_s)$ and U the number of unactivated surface sites (greys + greens).

Also from [20], the rate of deactivating a surface radical site (red block turning green or magenta block turning grey) is

$$\text{Deactivation rate (s}^{-1}\text{)} = k_2 [\text{H}]_s A \quad (5)$$

where $k_2 = 3.318 \times 10^{-11} \text{ cm}^3 \text{ s}^{-1}$ and A is the number of activated surface sites (reds + magentas).

Surface migration

The migration rate to be considered is that for an activated CH₂ bridging group to move along or across a dimer row. Netto & Frenklach [20] obtained a rate constant for these processes to be $\sim 1.5 \times 10^7 \text{ s}^{-1}$ (at $T_s = 900^\circ\text{C}$). More recently, Cheesman *et al.* [10] found the activation barrier for hopping to be slightly less than previously thought, with the values for moving along or across the dimer rows being 145.5 and 111.3 kJ mol⁻¹, respectively. Taking an average of these, and assuming the same pre-exponential factor as Netto & Frenklach, we obtain:

$$k_{\text{hop}} = 6.13 \times 10^{13} \exp(-128400 / RT_s) \quad (6)$$

for the rate constant of the pure hopping process. However, the activated CH₂ groups will only be able to hop if there is a suitable radical site in a neighbouring position. Previously, to obtain the overall rate of migration (per activated surface CH₂ group) we simply multiplied k_{hop} by the chance of a neighbouring site being a radical, typically 0.1. For our standard conditions, this gave values of the rate of migration to be $\sim 1.3 \times 10^7 \text{ s}^{-1}$, making migration the fastest process by far in the MC model. It also allowed the CH₂ group to migrate long distances (10-100 sites) across the surface before being etched or adding to the lattice.

However, there are problems with this simple model, since in reality the rate of migration may be significantly slowed by the lack of availability of surface radical sites. Thus, the migration rate is coupled to the H abstraction rate in a more complex way than we (and others) previously accounted for. The new model takes this into account by only allowing migration to occur if both the CH₂ is activated (red) *and* there is a neighbouring activated surface site (magenta) to receive it. One result of this new model for migration is that migrating red blocks hop back and forth rapidly between two adjacent radical sites, and only rarely migrate beyond this when a third surface site activates. Thus, the number of hops made by an individual red block was often of the order of 10^4 , but the average surface diffusion length was usually < 2 sites.

RESULTS and DISCUSSION

The modified program achieved its goals of simulating the growth of 300 layers of diamond in a few hours, with the morphology continuously evolving on the screen. Figure 3 shows plots of the diamond growth rate and the RMS roughness as a function of T_s for the HFCVD standard conditions, with all other conditions remaining constant. The simulation predicts an increasing growth rate with T_s , as seen in experiment. This is mainly due to an increase in the fraction of surface radical sites, which increases the adsorption rate. The RMS roughness decreases with T_s due to the increased migration of surface species.

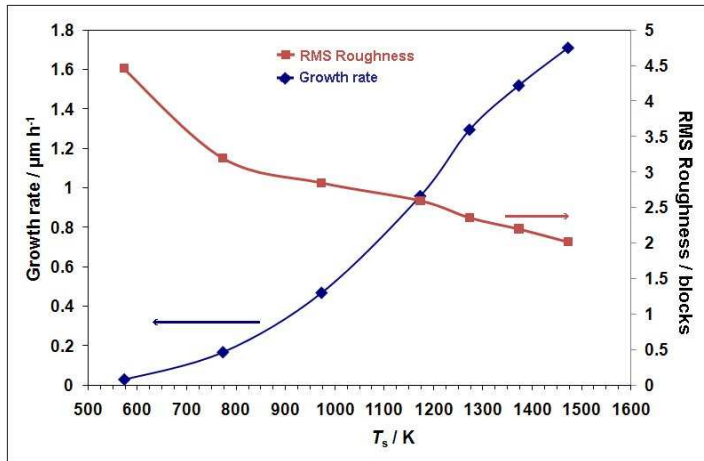


Figure 3. Diamond growth rate and RMS roughness calculated as a function of substrate temperature, T_s , for the standard HFCVD conditions.

The average diffusion length is defined as the mean distance that a migrating species ends up from its initial adsorption site when its migration is permanently terminated by processes such as etching, attachment to the lattice, *etc.* This diffusion length is a function of T_s (see figure 4), mainly through the increase in migration rate. However, the diffusion length remains very small, < 2.5 blocks (equivalent to surface lattice sites) for all temperatures tested. This shows that the major effect of migration is that migrating CH_2 species hop back and forth rapidly between two adjacent radical sites, and only rarely migrate beyond this when a third surface site activates adjacent to one of the previous two. Thus, the number of hops made by an individual red block was of the order of 10^4 , but the average surface diffusion distance remained < 2 sites.

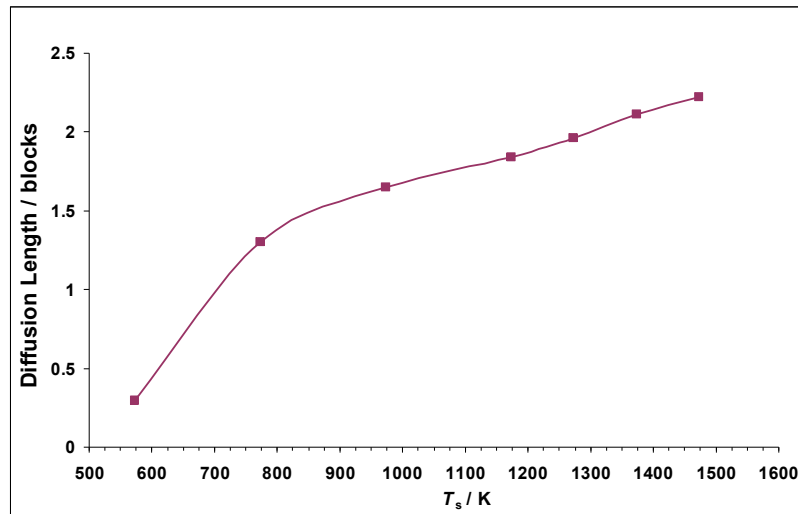


Figure 4. Average diffusion length (in blocks, equivalent to the C–C bond distance on the (100) surface) versus substrate temperature.

CONCLUSIONS

In this paper we have re-evaluated the rates for many of the fundamental steps involved in diamond growth, and which are then used for simulating growth in a KMC program. Etching is now believed to be a negligible process, since the excess energy dumped into the surface groups as a result of H addition can dissipate into the bulk before it can be used to break the C-C bond. This leaves β -scission as the only viable mechanism for removal of sp^3 carbon from a growing diamond surface. However, this process only etches <2% of the adsorbing species, meaning that the diamond growth rate is governed almost entirely by the arrival and sticking rate of carbons onto the surface. A major factor in this is the number of surface radical sites, and this value is governed by the $[H]/[H_2]$ ratio at the surface, as well as the surface temperature (or more accurately, the gas temperature near the surface). The other important factor – the impact rate for CH_3 species onto the surface – has been reduced to only 15% of that used previously, due to a combination of steric effects and electronic selection rules. This usefully decreases the predicted growth rate to values more in line with those seen in experiment. Migration is now seen as a much more complex process than previously believed, with the surface diffusion length being severely limited by the lack of availability of surface radical sites. Migrating CH_2 species can hop back and forth between two adjacent radical sites thousands of times before the migration process is terminated by processes such as the radical sites or CH_2 becoming deactivated, the CH_2 attaching to a sidewall, *etc.* Thus, the overall average surface diffusion length for a surface species is <2 sites, and this has implications for both the growth rate and the surface roughness.

In future work we shall explore these implications further and investigate the effect of different growth conditions, such as those used to grow SCD or UNCD, upon the predicted growth rates and growth rates and surface morphology.

ACKNOWLEDGMENTS

The authors wish to thank Mike Ashfold, Neil Fox, Keith Rosser, Ben Truscott, Walther Schwarzacher and Michael Frenklach for useful discussions and suggestions.

REFERENCES

1. P.W. May, *Science* **319**, 1490 (2008).
2. P.W. May, *Phil. Trans. Roy. Soc. Lond. A* **358**, 473 (2000).
3. D.G. Goodwin and J.E. Butler, in: M.A. Prelas, G. Popovici, L.K., Bigelow, Eds., *Handbook of Industrial Diamonds and Diamond Films* (Marcel Dekker, New York, 1998).
4. S. J. Harris, *Appl. Phys. Lett.* **56**, 2298 (1990).
5. J.E. Butler, R.L. Woodin, L.M. Brown, P. Fallon, *Phil. Trans. Roy. Soc: Phys. Sci. and Eng.* **342**, 209 (1993).
6. P.W. May, Yu.A. Mankelevich, *J. Phys. Chem. C* **112**, 12432 (2008).
7. P.W. May, N.L. Allan, J.C. Richley, M.N.R. Ashfold, Yu.A. Mankelevich, *J. Phys. Cond. Matter* **21**, 364203 (2009).
8. P.W. May, N.L. Allan, M.N.R. Ashfold, J.C. Richley, Yu.A. Mankelevich, *Diamond Relat. Mater.* (2010), in press (doi: 10.1016/j.diamond.2009.10.030).

9. S. Skokov, B. Weiner, M. Frenklach, *J. Phys. Chem.* **98**, 7073 (1994).
10. A. Cheesman, J.N. Harvey, M.N.R. Ashfold, *J. Phys. Chem. A*, **112**, 11436 (2008).
11. J.C. Richley, J.N. Harvey and M.N.R. Ashfold, *J. Phys. Chem. A* **113**, 11416 (2009).
12. K. Larsson, J.-O. Carlsson, *phys. stat. sol. (a)* **186**, 319 (2001).
13. J.C. Richley, J.N. Harvey, M.N.R. Ashfold, Poster J17.32, *Proc. MRS Fall Meeting* 2009.
14. A.B. Bortz, M.H. Kalos, J.L. Lebowitz, *J. Comp. Phys.* **17**, 10 (1975).
15. Yu.A. Mankelevich, M.N.R. Ashfold, J. Ma, *J. Appl. Phys.* **104**, 113304 (2008).
16. T. Van Regemorter, K. Larsson, *J. Phys. Chem. A* **112**, 5429 (2008).
17. S.J. Klippenstein, Y. Georgievskii, L.B. Harding, *Phys. Chem. Chem. Phys.* **8**, 1133 (2006).
18. R.E. Rawles, S.F. Komarov, R. Gat, W.G. Morris, J.B. Hudson, M.P. D'Evelyn, *Diamond Relat. Mater.* **6**, 791 (1997).
19. R.E. Stallcup II, J.M. Perez, *Phys. Rev. Letts.* **86**, 3368 (2001).
20. A. Netto, M. Frenklach, *Diamond Relat. Mater.* **14**, 1630 (2005).
21. M. Frenklach, S. Skokov, *J. Phys. Chem. B* **101**, 3025 (1997).
22. C.M. Donnelly, R.W. McCullough, J. Geddes, *Diamond Relat. Mater.* **6**, 787 (1997).
23. C.C. Battaile, D.J. Srolovitz, *Annu. Rev. Mater. Res.* **32**, 297 (2002).